Letter

Uncovering the mystery of $X(3872)$ with the coupled-channel dynamics

Jun-Zhang Wang,[1,2,*] Zi-Yang Lin,[1,†] Yan-Ke Chen,[1,‡] Lu Meng,[3,§] and Shi-Lin Zhu[1,‖]

[1]*School of Physics and Center of High Energy Physics, Peking University, Beijing 100871, China*
[2]*Department of Physics, Chongqing University, Chongqing 401331, China*
[3]*Institut für Theoretische Physik II, Ruhr-Universität Bochum, D-44780 Bochum, Germany*

(Received 29 June 2024; accepted 6 June 2025; published 25 June 2025)

The $X(3872)$, as the first and the most crucial member in the exotic charmoniumlike XYZ family, has been studied for a long time. However, its dynamical origin, whether stemming from a $D\bar{D}^*$ hadronic molecule or the first excited P-wave charmonium $\chi_{c1}(2P)$, remains controversial. In this Letter, we demonstrate that the $X(3872)$ definitely does not result from the mass shift of the higher bare $\chi_{c1}(2P)$ resonance pole in the coupled-channel dynamics involving a short-distance $c\bar{c}$ core and the long-distance $D\bar{D}^*$ channels. Instead, it originates from either the $D\bar{D}^*$ molecular pole or the shadow pole associated with the antiresonance of the P-wave charmonium, depending on the weak or strong coupling mode, respectively. To differentiate these origins and fully exploit the nature of $X(3872)$, we conduct a comprehensive analysis in a couple-channel dynamics framework, including the isospin violation, the three-body $D\bar{D}\pi$ effect, the dynamical width of D^*, and nonopen-charm decays of the bare $\chi_{c1}(2P)$. Our findings highlight the pivotal role of the coupled-channel dynamics in explaining the disparity between the pole widths of $X(3872)$ and T_{cc}^+, while also predicting a new resonance with $J^{PC}=1^{++}$ around 4.0 GeV. By matching the newly observed $\chi_{c1}(4010)$ by the LHCb Collaboration to our predicted resonance, we conclude that the $X(3872)$ most likely originates from the $D\bar{D}^*$ pole with a confidence level exceeding 99.7%.

DOI: 10.1103/929g-cv15

Introduction. Over the past two decades, one of the central challenges in the strong interaction physics is to understand numerous exotic XYZ resonances (see Refs. [1–6] for recent progresses). As the undisputed superstar among them, the nature of $X(3872)$ is the most mysterious, which is mainly manifested in that its mass exactly coincides to the threshold of $D^0\bar{D}^{*0}/D^{*0}\bar{D}^0$ and its decay pattern exhibits a strong coupling to the $D^0\bar{D}^0\pi^0$ final state [7,8]. These distinctive features imply the central role of the $D\bar{D}^*$ (specifically refers to $D\bar{D}^*/\bar{D}D^*$) interaction in the generation of $X(3872)$, leading to the natural proposal of a hadronic molecular interpretation of $X(3872)$ [9–14]. In a related development, the LHCb Collaboration recently discovered the doubly charmed tetraquark T_{cc}^+ in the prompt production of the pp collision [15,16], which has been widely recognized as an ideal candidate for a shallow DD^* bound state [17–42].

In contrast to the doubly charmed tetraquark T_{cc}^+, the nature of $X(3872)$ presents a more intricate challenge, as its $D\bar{D}^*$ component inevitably interacts with the conventional charmonium states with the same quantum number $J^{PC}=1^{++}$ [43,44], most notably the nearby $\chi_{c1}(2P)$ state (hereinafter denoted as χ_{c1}'). This dynamics indicates that the realistic wave function of $X(3872)$ exhibits dual characteristics: a compact charmonium in the short-distance region and a loose $D\bar{D}^*$ structure in the long-distance region [45–48]. In light of this, a widely held opinion suggests that the $X(3872)$ arises from the mass shift of the higher bare χ_{c1}' state, driven by the unquenched $D\bar{D}^*$ loop correction to the propagator of the P-wave charmonium [49–55]. Consequently, whether the $X(3872)$ is a hadronic molecule or an excited charmonium remains controversial. Regarding this long-standing view, in this letter, we demonstrate that the $X(3872)$ definitely does not originate from the bare χ_{c1}' resonance pole in the coupled-channel dynamics involving the $c\bar{c}$ core and the $D\bar{D}^*$ channels. In contrast, the $X(3872)$ stems from either the $D\bar{D}^*$ pole in the so-called weak-coupling mode or the shadow pole associated with antiresonance of charmonium in the strong-coupling mode. Therefore, our research has rectified the misunderstanding regarding the pole origin of $X(3872)$ in previous literature [49–55] and concluded that the conventional charmonium explanation of $X(3872)$ can be ruled out.

*Contact author: wangjzh2022@pku.edu.cn
†Contact author: lzy_15@pku.edu.cn
‡Contact author: chenyanke@stu.pku.edu.cn
§Contact author: lu.meng@rub.de
‖Contact author: zhusl@pku.edu.cn

Published by the American Physical Society under the terms of the Creative Commons Attribution 4.0 International license. Further distribution of this work must maintain attribution to the author(s) and the published article's title, journal citation, and DOI. Funded by SCOAP³.

To fully understand the nature of $X(3872)$, we perform a coupled-channel dynamical calculation, incorporating the $D\bar{D}^*$ interaction via the chiral effective field theory (ChEFT) and three key mechanisms contributing to the pole width of $X(3872)$: the $D\bar{D}\pi$ three-body cut from the one-pion exchange (OPE) in $D\bar{D}^*$ scattering, the dynamical width of $\bar{D}^*$ and the nonopen-charm decays of the bare χ'_{c1} state. A notable prediction is the existence of a new resonance with $J^{PC} = 1^{++}$ around 4.0 GeV when the $X(3872)$ pole emerges. Remarkably, we establish a quantitative connection among the dynamical origin of $X(3872)$, its pole width and the properties of this predicted resonance, which offers a novel approach to distinguish the origins of $X(3872)$. Thanks to the LHCb observation of $\chi_{c1}(4010)$ and given our assumptions of $\chi_{c1}(4010)$ as the predicted new resonance, we conclude with over 99.7% confidence that $X(3872)$ originates from the $D\bar{D}^*$ pole. Our findings demonstrate the irreplaceable role of coupled-channel dynamics in unlocking the mystery of $X(3872)$, while providing important implications for understanding other XYZ states.

Pole evolution of $X(3872)$ in the coupled-channel dynamics. We adopt a coupled-channel framework to study the properties of $X(3872)$, in which the $D\bar{D}^*$ scattering dynamics is also included. The hadronic Fock state can be written as

$$|\Phi\rangle = c_0|\Phi_0\rangle + \sum_i \int \frac{d^3\mathbf{q}}{(2\pi)^3}\phi_i(\mathbf{q})|\Phi_i\rangle_{\mathbf{q}}, \tag{1}$$

where $|\Phi_0\rangle$ and $|\Phi_i\rangle_{\mathbf{q}}$ correspond to the bare Fock state and the i-channel hadron-hadron continuum associated with the relative momentum $\mathbf{q}$, respectively. Due to poor knowledge of the compact tetraquark $[c\bar{c}q\bar{q}]$ spectrum in the present theoretical investigations, it seems rather unlikely that we will explore the role of this bare Fock state in the coupled channel dynamics associated with the formation of $X(3872)$. In order to clearly identify this point, more experimental hints and evidence from lattice QCD are needed. Then the coupled-channel Schrödinger equation can be written as

$$\begin{pmatrix} \mathcal{H}_0 & \mathcal{H}_{01} & \mathcal{H}_{02} & \cdots \\ \mathcal{H}_{10} & \mathcal{H}_1 & \mathcal{H}_{12} & \cdots \\ \mathcal{H}_{20} & \mathcal{H}_{21} & \mathcal{H}_2 & \cdots \\ \vdots & \vdots & \vdots & \ddots \end{pmatrix} \begin{pmatrix} c_0|\Phi_0\rangle \\ |\Phi_1\rangle \\ |\Phi_2\rangle \\ \vdots \end{pmatrix} = E \begin{pmatrix} c_0|\Phi_0\rangle \\ |\Phi_1\rangle \\ |\Phi_2\rangle \\ \vdots \end{pmatrix} \tag{2}$$

with

$$|\Phi_i\rangle = \int \frac{d^3\mathbf{q}}{(2\pi)^3}\phi_i(\mathbf{q})|\Phi_i\rangle_{\mathbf{q}}, \qquad (i = 1, 2, \ldots). \tag{3}$$

After expanding the above matrix equation and applying the relation $\langle\Phi_0|\mathcal{H}_0|\Phi_0\rangle = M_0$, $\langle\Phi_j|_{\mathbf{q}}\mathcal{H}_{j0}|\Phi_0\rangle = \mathcal{V}_{0j}(\mathbf{q})$, and $\langle\Phi_j|_{\mathbf{q}'}\mathcal{H}_{ji}|\Phi_i\rangle_{\mathbf{q}} = \delta_{ij}E_k + V_{ij}(\mathbf{q},\mathbf{q}')$, one can obtain

$$\sum_i \int \phi_i(\mathbf{q})\mathcal{V}_{i0}(\mathbf{q})\frac{d^3\mathbf{q}}{(2\pi)^3} = (E - M_0)c_0, \tag{4}$$

$$c_0\mathcal{V}_{0j}(\mathbf{q}) + \sum_i \int (\delta_{ij}E_k + V_{ij}(\mathbf{q},\mathbf{q}'))\phi_i(\mathbf{q}')\frac{d^3\mathbf{q}'}{(2\pi)^3} = E\phi_j(\mathbf{q}) \qquad (j = 1, 2, 3\ldots), \tag{5}$$

respectively, where M_0 is the bare mass of $|\Phi_0\rangle$, the $\mathcal{V}_{0j}$ corresponds to the transition amplitude between the bare state and the jth channel, and the E_k and V_{ij} stand for the kinetic term $\mathbf{q}^2/(2\mu)$ and the potential of the corresponding hadron-hadron scattering, respectively. Combining Eqs. (4) and (5), we have

$$\sum_i \left(\delta_{ij}E_k + \int (V_{ij}(\mathbf{q},\mathbf{q}') + \mathcal{V}_{ij}(\mathbf{q},\mathbf{q}'))\phi_i(\mathbf{q}')\frac{d^3\mathbf{q}'}{(2\pi)^3}\right) = E\phi_j(\mathbf{q}) \qquad (j = 1, 2, 3\ldots), \tag{6}$$

where $\mathcal{V}_{ij}(\mathbf{q},\mathbf{q}') = \frac{\mathcal{V}_{i0}(\mathbf{q}')\mathcal{V}_{0j}(\mathbf{q})}{E - M_0 + i\epsilon}$. Equation (6) is a standard coupled-channel Schrödinger equation in momentum space. The coupled-channel problem between the bare state and the hadronic continuum is converted to a hadron-hadron scattering problem including an extra s-channel effective potential $\mathcal{V}_{ij}(\mathbf{q},\mathbf{q}')$.

We consider a two-channel calculation involving the $[D^0\bar{D}^{*0}]$ and $[D^+\bar{D}^{*-}]$, where the square brackets are the shorthand of the $C = +$ states such as $[D^0\bar{D}^{*0}] = \frac{1}{\sqrt{2}}(D^0\bar{D}^{*0} - \bar{D}^0D^{*0})$. Because the mass of $X(3872)$ lies close to the threshold of $D^0\bar{D}^{*0}$, the $D\bar{D}^* \to D\bar{D}^*$ scattering should be governed by the leading-order contact and OPE interactions in the effective field theory [28]. The total effective potential can be written as

$$V_{\text{Total}}(\mathbf{q},\mathbf{q}') = \begin{pmatrix} C_t - V_{\pi^0} + \mathcal{V}_{11} & C'_t - 2V_{\pi^\pm} + \mathcal{V}_{12} \\ C'_t - 2V_{\pi^\pm} + \mathcal{V}_{21} & C_t - V_{\pi^0} + \mathcal{V}_{22} \end{pmatrix}, \tag{7}$$

where C_t and C'_t are the contact terms, V_π is the OPE potential and $\mathcal{V}_{11} = \mathcal{V}_{12} = \mathcal{V}_{21} = \mathcal{V}_{22}$. Since the ChEFT only works at small momentum, we introduce a Gaussian cutoff to regularize the contact and OPE potential, i.e.,

$$\mathcal{F}(\mathbf{q},\mathbf{q}') = \exp(-(\mathbf{q}^2 + \mathbf{q}'^2)/\Lambda^2), \tag{8}$$

where the cutoff $\Lambda = 0.5$ GeV is usually taken for the DD^* or $D\bar{D}^*$ system [28]. In order to explore the trajectory of the pole generated in the $D\bar{D}^* \to D\bar{D}^*$ scattering, we first ignore the OPE contribution and adopt the momentum-dependent form of

$$\mathcal{V} = \frac{g^2}{2M_0} e^{-(\mathbf{q}^2+\mathbf{q}'^2)/\alpha^2}/(E - M_0 + i\epsilon), \tag{9}$$

where α and g characterize the coupling range and strength between χ'_{c1} and $D\bar{D}^*$, respectively. Then the effective potential in Eq. (7) becomes separable, and it would be very convenient to analytically solve the Lippmann-Schwinger equation (LSE) and search for the poles of the T matrix [56].

The general coupled-channel LSE is given by

$$T^{\alpha}_{\beta}(q,q') = V^{\alpha}_{\beta}(q,q') + \sum_{\gamma} \int_0^{\infty} \frac{dkk^2}{(2\pi)^3} \frac{V^{\alpha}_{\gamma}(q,k) T^{\gamma}_{\beta}(k,q')}{E - k^2/(2\mu_{\gamma})}, \tag{10}$$

where $V^{\alpha}_{\beta}(q,q')$ is the partial-wave-projected potential from the α channel to the β channel, and q and q' correspond to the initial and final momentum, respectively. The reduced mass $\mu_{\gamma}=m_1 m_2/(m_1+m_2)$.

We first focus on the situation with the strict isospin symmetry, in which the two-channel calculation in Eq. (10) is reduced to a single-channel one. The pole trajectories of the $D\bar{D}^*$ scattering in the momentum k_0-plane when increasing the coupling strength g are presented in Fig. 1. Here, k_0 is defined by $k_0 = \sqrt{2\mu(E - m_D - m_{D^*})}$. k_0 with positive and negative imaginary parts correspond to the first and second Riemann sheets of the T matrix, respectively. The bare mass $M_0 = 3.96$ GeV is adopted according to the quark model estimations [57,58]. Figures 1(a) and 1(b) with no contact interaction ($C_t = 0$ GeV^{-2}) corresponds to the so-called weak coupling mode with a typical value $\alpha = 1.0$ GeV and in the strong coupling mode with $\alpha = 1.4$ GeV, respectively, which indicates a smaller and larger overlap range between the wave functions of the $c\bar{c}$ core and $D\bar{D}^*$ channel.

In the weak coupling mode, there appear three poles of the T matrix in the complex plane, although only the s-channel interaction $\mathcal{V}$ is considered. It is easy to identify the nature of these three poles by setting $g^2 \to 0$. The red, blue and green poles correspond to the bare χ'_{c1} resonance, the shadow pole associated with χ'_{c1} resonance and a virtual state of $D\bar{D}^*$ at the infinity, respectively. With gradually increasing g^2, the pole of χ'_{c1} resonance moves first toward and then away from the threshold of $D\bar{D}^*$, while the $D\bar{D}^*$ virtual state continuously moves toward the threshold and finally crosses the unitary branch cut of $D\bar{D}^*$ and becomes a bound state, which corresponds to the observed $X(3872)$ structure. For the strong coupling mode shown in Fig. 1(b), the situation is completely different. When g^2 increases to a critical value, the χ'_{c1} pole and its shadow pole will meet at the same point as virtual states and then continue to move along the negative imaginary axis of the k_0-plane in opposite directions. Subsequently, the χ'_{c1} pole will meet the $D\bar{D}^*$ virtual state pole arising from the infinity and then

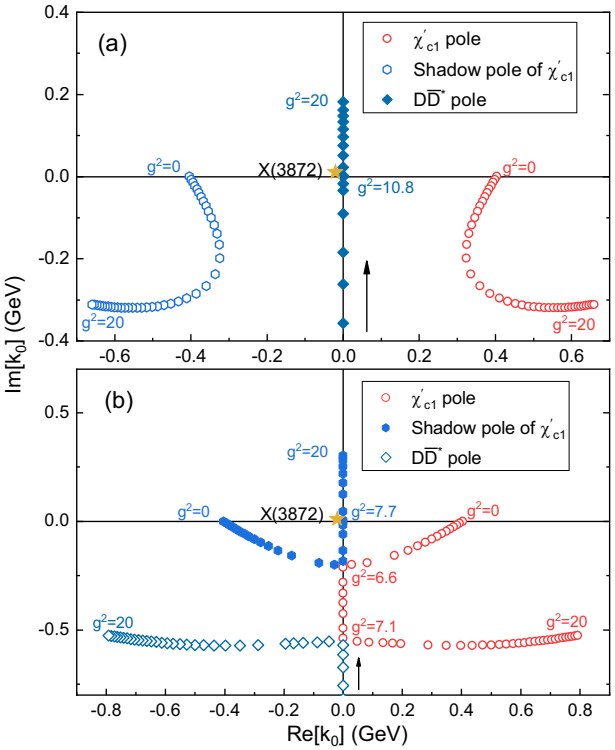


FIG. 1. The pole evolutions of the single-channel $D\bar{D}^* \to D\bar{D}^*$ scattering in the coupled-channel dynamics. Here, the complex plane refers to the momentum k_0. Figure (a) and (b) correspond to a typical value of $\alpha = 1.0$ GeV and $\alpha = 1.4$ GeV, respectively.

they evolve into a pair of resonance and antiresonance. In contrast, the shadow pole associated with χ'_{c1} enters the first Riemann sheet and is related to a $X(3872)$ state.

It is important to highlight that this pole separation behavior associated with the χ'_{c1} state is directly attributed to the tiny imaginary part $i\epsilon$ of the effective potential

$$\mathcal{V} \propto (m_{\rm th} + k_0^2/(2\mu) - M_0 + i\epsilon)^{-1}. \tag{11}$$

Thus, such a phenomenon is still universal when including the intrinsic $D\bar{D}^*$ dynamics, as shown in Supplemental Material (SM) [59]. It can be concluded that an intrinsic attractive force between D and $\bar{D}^*$ prompts the pole evolution behaviors to favor the weak coupling mode and a repulsive force causes poles to evolve in favor of the strong coupling mode. To sum up, whatever the dynamics origin of $X(3872)$ is, $X(3872)$ *does not originate from the mass shift of the bare* χ'_{c1} *resonance pole in the coupled-channel dynamics.*

For $X(3872)$, the isospin breaking effect is significant since the mass difference between the neutral and charged channels is up to 8 MeV [60]. Thus, we further study the pole evolution of $D\bar{D}^* \to D\bar{D}^*$ in the two-channel scattering, which is presented in Fig. 2. Here, in order to make the T-matrix a single-valued function in the locally flat surface, a uniformization variable z is introduced to achieve a

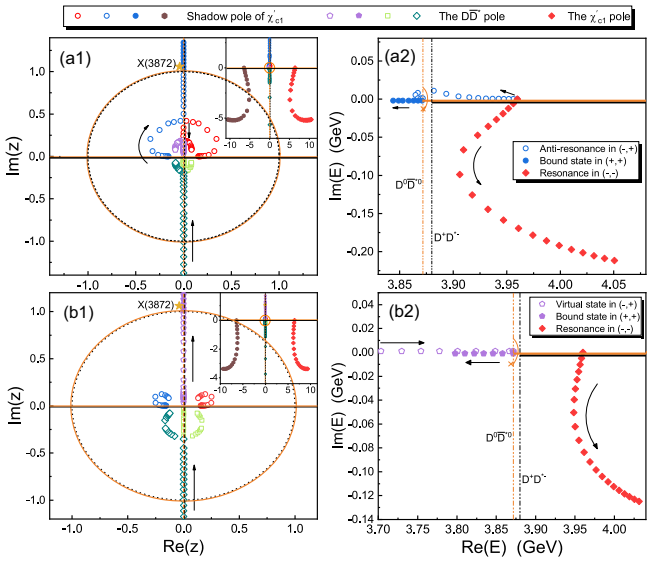


FIG. 2. The pole evolutions of the two-channel $D\bar{D}^* \to D\bar{D}^*$ scattering (isospin violation) in the coupled-channel dynamics. Left and right figures are related to the uniformization z-plane and the corresponding energy E-plane. It is worth emphasizing that the solid and hollow blue (purple) points refer to the same pole. Figures (a1)/(a2) and (b1)/(b2) correspond to a strong coupling mode ($\alpha = 1.0$ GeV) and a weak coupling mode ($\alpha = 0.8$ GeV), respectively."

mapping from energy E to z [74–76], whose definition is summarized in the SM [59]. In the z/E-plane of Fig. 2, the orange and black solid lines stand for the unitary branch cuts related to the $[D^0\bar{D}^{*0}]$ and $[D^+\bar{D}^{*-}]$, respectively. The dashed lines represent the real axis of the E-plane unoccupied by the branch cut. The four Riemann sheets $(+,+)$, $(-,+)$, $(+,-)$, and $(-,-)$ for the two-channel system correspond to the upper half z-plane outside and inside the circle, and the lower half z-plane inside and outside the circle, respectively, where $+$ and $-$ represent the first and the second Riemann sheets, respectively.

Since the impact of the intrinsic $D\bar{D}^*$ dynamics on the pole evolution in the two-channel case is very similar to the lesson learned from the single-channel analysis, here we only show the two-channel calculations with $C_t = C'_t = 0$ GeV^{-2}. In Fig. 2(a1) with a typical value $\alpha = 1.0$ GeV, a large number of new poles appear due to the isospin symmetry violation, and it can be found that the evolution behaviors of the dressed χ'_{c1} resonance and its shadow pole in the $(-,-)$ sheet are very similar to those of the weak coupling mode in the single-channel case. However, the $X(3872)$ pole no longer arises from the virtual $D\bar{D}^*$ state in the $(-,-)$ sheet. Instead, it arises from the shadow resonance of χ'_{c1} in the $(-,+)$ sheet. In Fig. 2(a2), we show the corresponding pole trajectories in the complex energy plane. It can be seen that the dressed χ'_{c1} resonance is always higher than the $[D^+\bar{D}^{*-}]$ threshold. Its shadow pole in the $(-,+)$ sheet first moves into the energy region below the $[D^0\bar{D}^{*0}]$ threshold and then returns and

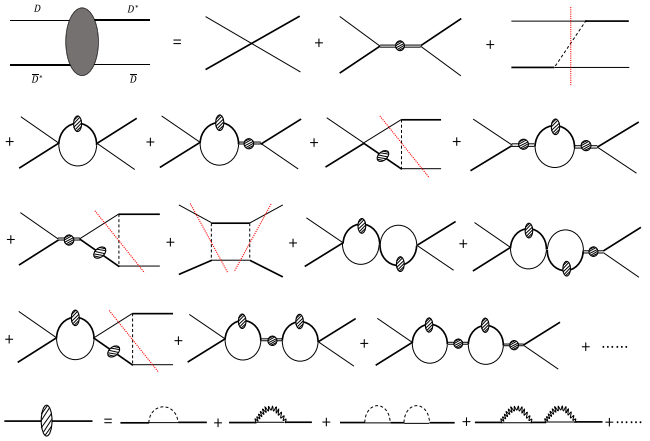


FIG. 3. The full Feynman diagram of the $D\bar{D}^* \to D\bar{D}^*$ scattering in the coupled-channel dynamics. The self-energy diagram from the nonopen-charm decays for the bare χ'_{c1} is marked by shadow circle.

crosses the unitary cut of $[D^0\bar{D}^{*0}]$ into the $(+,+)$ sheet and becomes a bound state $X(3872)$. This trajectory is still maintained when employing a stronger coupling mode such as $\alpha = 1.4$ GeV. However, when adopting a weaker coupling mode ($\alpha = 0.8$ GeV), as presented in Figs. 2(b1) and 2(b2), the shadow pole of χ'_{c1} in the $(-,+)$ sheet will not be pulled to the imaginary axis of the z-plane and the $X(3872)$ originates from a $D\bar{D}^*$ virtual state pole in the $(-,+)$ sheet.

A novel approach to reveal the nature of $X(3872)$. Recently, the LHCb and BESIII Collaborations extracted the pole position of $X(3872)$ by analyzing the line shape, whose imaginary parts are $-(130^{+320}_{-180})i$ keV [61] and $-(190^{+206}_{-161})i$ keV [62], respectively. Both of the center absolute values are obviously larger than $-(24 \pm 1)i$ keV [15,16] of T^+_{cc}. The pole width of T^+_{cc} has been reproduced well in theoretical calculations, attributed mainly to its three-body $DD\pi$ decay [26–29,31]. However, the $D\bar{D}\pi$ half decay width of $X(3872)$ from the three-body cut of the OPE potential is estimated to be only 15–34 keV in Refs. [28,29], and the reason for the large pole width of $X(3872)$ remains unclear in the current theoretical studies.

Here, we perceive that the coupled-channel dynamics plays a key role in the large pole width of $X(3872)$. This idea is supported by the fact that the experimental total width of the ground state charmonium $\chi_{c1}(1P)$ without open-charm decay channels, can reach 0.88 ± 0.05 MeV [60]. Hence, it is reasonable to expect that the nonopen-charm decay widths of the bare χ'_{c1} state are of a similar order of magnitude. We employ a quark-model-independent scheme to estimate the decay behaviors of the bare χ'_{c1} state. The relevant details can be found in the SM [59]. The coupling amplitude $\mathcal{V}_{0j}(\mathbf{q})$ and $\mathcal{V}_{i0}(\mathbf{q}')$ in Eq. (6) can also be obtained in the quark pair creation

TABLE I. The poles and component possibilities[a] of $X(3872)$ and a new resonance in the complete coupled-channel dynamics. The pole of $X(3872)$ is given by the binding energy relative to the $D^0\bar{D}^{*0}$ threshold. The χ and M superscripts denote the dressed χ'_{c1} resonance and the distorted $D\bar{D}^*$ resonance in the $(-,-)$ sheet, respectively. Here, $V_{ct}^{I=1} = 0$ GeV^{-2} and all pole positions are in units of MeV. It is important to emphasize that, while the real part of the experimentally extracted pole for $X(3872)$ is slightly positive, it remains on the first Riemann sheet. In this analysis, we compare the experimental results with a theoretical bound-state pole whose real part is slightly negative. This difference does not compromise the validity of the comparison, as such a pole can be continuously shifted above the threshold, staying on the same Riemann sheet, through a slight reduction in the interaction strength.

λ ($V_{ct}^{I=0}$) GeV^{-1} (GeV^{-2})			0.5 (96.6)	1.0 (22.5)	1.25 (11.2)	1.5 (3.7)	2.5 (−13.1)
Without $\Gamma_a + \Gamma_b$	$X(3872)$	Pole	$-0.086 - 0.003$i	$-0.140 - 0.024$i	$-0.097 - 0.027$i	$-0.089 - 0.029$i	$-0.075 - 0.030$i
With $\Gamma_a + \Gamma_b$	$X(3872)$	Pole	$-0.059 - 1.36$i	$-0.060 - 0.293$i	$-0.060 - 0.164$i	$-0.070 - 0.119$i	$-0.071 - 0.065$i
		$\mathcal{P}_{D^0\bar{D}^{*0}}$	$0.145 - 0.015$i	$0.748 - 0.136$i	$0.858 - 0.078$i	$0.895 - 0.047$i	$0.939 - 0.013$i
		$\mathcal{P}_{D^+\bar{D}^{*-}}$	$0.110 + 0.002$i	$0.092 + 0.049$i	$0.065 + 0.035$i	$0.056 + 0.024$i	$0.043 + 0.009$i
		$\mathcal{P}_{\chi'_{c1}}$	$0.745 + 0.013$i	$0.160 + 0.087$i	$0.077 + 0.043$i	$0.049 + 0.023$i	$0.018 + 0.004$i
	New resonance	Pole	$4150 - 141$i^M	$4063 - 129$i^M	$4025 - 92$i$^\chi$	$4004 - 57$i$^\chi$	$3977 - 8$i$^\chi$
		$\mathcal{P}_{D^0\bar{D}^{*0}}$	$0.328 + 0.048$i	$0.278 - 0.191$i	$0.203 - 0.255$i	$0.104 - 0.209$i	$0.088 - 0.040$i
		$\mathcal{P}_{D^+\bar{D}^{*-}}$	$0.324 + 0.007$i	$0.265 - 0.219$i	$0.187 - 0.286$i	$0.086 - 0.234$i	$0.092 - 0.062$i
		$\mathcal{P}_{\chi'_{c1}}$	$0.348 - 0.055$i	$0.457 + 0.410$i	$0.610 + 0.541$i	$0.810 + 0.443$i	$0.820 + 0.102$i
BESIII [62]		Pole	$(0.0068^{+0.1655}_{-0.1700}) - (0.190^{+0.206}_{-0.161})i$				
LHCb [61]		Pole	$(0.06^{+0.16}_{-0.16}) - (0.13^{+0.32}_{-0.18})i$				

[a]Here, the component possibility $\mathcal{P}$ is defined as $\mathcal{P}_i = (\phi_i|\phi_i)$ with the wave function of ith channel ϕ_i, which roughly reflects the ratio of the ith channel. For the non-Hermitian system, the wave function normalization is defined by c-product [83,84], which means $(\phi|\phi) = \sum_i \int \frac{dp^3}{(2\pi)^3} e^{-3i\theta}\phi_i(\tilde{\boldsymbol{p}})^2 = 1$, where θ is the rotation angle in complex scaling method, and subscript i represents the involved channels.

(QPC) model without extra parameter dependence. Now, the s-channel effective potential should be modified as

$$\mathcal{V}_{ij}(\mathbf{q},\mathbf{q}') = \frac{\mathcal{V}_{i0}(\mathbf{q}')\mathcal{V}_{0j}(\mathbf{q})}{E - M_0 + i\epsilon} \to \frac{\mathcal{V}_{i0}(\mathbf{q}')\mathcal{V}_{0j}(\mathbf{q})e^{-\lambda^2(\mathbf{q}^2+\mathbf{q}'^2)}}{E - M_0 + i\frac{1}{2}(\Gamma_a + \Gamma_b)}, \tag{12}$$

where $\Gamma_a = 3488$ keV and $\Gamma_b = 220$ keV correspond to the light hadron decays and radiative decays of the bare χ'_{c1}, respectively. According to suggestions from Refs. [77–79], an extra cutoff parameter λ is required to adjust the large momentum suppression in $\mathcal{V}_{i0}$ from the input of the QPC amplitude. Additionally, we also simultaneously take into account the three-body $D\bar{D}\pi$ threshold effect from the OPE interaction [28] and the dynamical width of $\bar{D}^*$ from its strong decay $\bar{D}\pi$ and electromagnetic decay $\bar{D}\gamma$. The complete scattering amplitudes of $D\bar{D}^* \to D\bar{D}^*$ involving these three potential mechanisms contributing to the pole width are presented in Fig. 3.

The inclusion of these decay dynamics makes the system Hamiltonian no longer Hermitian. In this situation, a more convenient approach to extract the pole positions with the full scattering amplitudes in Fig. 3 is the complex scaling method (CSM) [80–82]. In our previous studies on T_{cc}^+ with ChEFT [28], the pole width is not sensitive to the cutoff Λ within a large range $\Lambda = 0.4$–1.0 GeV, and then the Λ cutoff dependence can be safely canceled by renormalizing the contact interaction. Thus, the Λ is fixed to 0.5 GeV and the undetermined parameters are λ, C_t, and C'_t. The last two can be related to two new contact constants $V_{ct}^{I=0}$ and $V_{ct}^{I=1}$ (see SM for their definitions [59]). First, we ignore the isospin violation of the contact interaction, i.e., $V_{ct}^{I=1} = 0$. The solved observable poles and their corresponding component possibilities are listed in Table I. For different cutoff values λ, we adjust $V_{ct}^{I=0}$ in a one-to-one manner to match the small binding energy of $X(3872)$. When only the width $\Gamma_a + \Gamma_b$ from the bare state is involved, whose contribution can be transferred into other poles via the coupled-channel mechanism, the pole width of $X(3872)$ can be significantly enlarged to the order of $\mathcal{O}(10^{-1})$ MeV, which highlights the crucial role of coupled-channel dynamics.

As a notable prediction, a higher resonance pole is found around 4 GeV as shown in Table I, which corresponds either to the genuine dressed charmonium χ'_{c1} resonance as argued in Refs. [85–91] or to a distorted $D\bar{D}^*$ resonance. In the latter case, the χ'_{c1} resonance evolves into a virtual pole far from the physical area in the $(-,-)$ sheet. Interestingly, we find that the pole width of $X(3872)$ and the properties of the new resonance are highly sensitive to the cutoff λ, with its variation from small to large values directly reflecting the transition from strong to weak coupling modes, as introduced in the previous section. For instance, for $\lambda = 0.5$ GeV^{-1}, the $X(3872)$ pole originates from the shadow resonance of χ'_{c1} in the $(-,+)$ sheet, whereas for $\lambda = 2.5$ GeV^{-1}, it corresponds to the $D\bar{D}^*$ pole in the

same sheet. Additionally, as shown in Table I, poles with a larger $c\bar{c}$ component typically correspond to strong coupling mode. Conversely, poles with a dominant $D\bar{D}^*$ component tend to correspond to a weak coupling mode. The results assuming an evident isospin violation of the contact interaction are summarized in the SM [59], in which the similar conclusions are obtained. This remarkable feature inspires a new idea: the characteristic physical quantity of $X(3872)$—pole width or the predicted new resonance can be treated as a novel indicator to convincingly reveal the nature of $X(3872)$. In particular, a very narrow pole width of $X(3872)$ on the order of tens of keV, similar to that of $T_{cc}(3875)$, strongly implies a dominant molecular composition of $X(3872)$ and the origin of the $D\bar{D}^*$ pole. On the other hand, an imaginary part of the $X(3872)$ pole in the hundreds of keV to MeV would suggest a significant compact $c\bar{c}$ admixture and favor the origin of the shadow pole of χ'_{c1}. Unfortunately, due to current experimental precision limitations, the imaginary part of the $X(3872)$ pole is still not well determined. Future high-precision measurements could serve as a powerful discriminator for the internal structure of $X(3872)$.

Thanks to the recent LHCb observation of $\chi_{c1}(4010)$, determined with an exceptionally high statistical significance (16σ) through a new amplitude analysis involving simultaneous fits to two C-parity-related decays $B^+ \to D^+D^{*-}K^+$ and $B^+ \to D^-D^{*+}K^+$ [63], our prediction is strongly validated. Here, it is worth emphasizing that the $B \to D\bar{D}^*K$ is a complicated decay process and the reported $\chi_{c1}(4010)$ state is still single observation, which requires further confirmation by other experiments. If we assume that the $\chi_{c1}(4010)$ state exists, for the following three reasons, the identification of $\chi_{c1}(4010)$ as our predicted resonance is highly reasonable. First, the $\chi_{c1}(4010)$ was observed in the invariant mass spectrum of $D^{*\pm}D^{\mp}$, the dominant decay mode of our predicted resonance. Second, although its mass lies close to the threshold of $D^*\bar{D}^*$, the existence of an S-wave $D^*\bar{D}^*$ structure with $J^{PC} = 1^{++}$ is forbidden due to the odd C-parity constraint for particle-antiparticle systems. Third, higher P-wave charmonium excitations are significantly beyond the mass range of $\chi_{c1}(4010)$, for example the $\chi_{c1}(3P)$, which was widely predicted to reside around 4.3 GeV [57,58]. These factors make alternative explanations for $\chi_{c1}(4010)$ highly unlikely. We match our predicted resonance to the newly observed $\chi_{c1}(4010)$ and present the experimental constraints incorporated in two-dimension Gaussian distribution function on parameter λ, with detailed results shown in the SM [59]. Although current experimental information on the pole width of $X(3872)$ does not distinguish its two pole origins, the $\chi_{c1}(4010)$ imposes strong constraints on the coupling modes of the coupled-channel dynamics. Ultimately, we conclude with over 99.7% confidence level that $X(3872)$ originates from the $D\bar{D}^*$ pole in the $(-,+)$ Riemann sheet.

Summary. We have studied the pole origin of $X(3872)$ with the coupled-channel dynamics and definitely demonstrated that the $X(3872)$ does not originate from the mass shift of the bare χ'_{c1} resonance pole. Accordingly, it stems from either the $D\bar{D}^*$ virtual state pole in the weak-coupling mode or the shadow pole associated with χ'_{c1} in the strong-coupling mode. Furthermore, we focused on the pole width of $X(3872)$ by considering the complete scattering dynamics, incorporating three key dynamical mechanisms. Our findings indicate that the coupled-channel dynamics will result in an apparently larger pole width of $X(3872)$. More intriguingly, we have established a quantitative connection among the dynamical origin of $X(3872)$, its pole width and the properties of the predicted new resonance. This underscores the importance of precisely measuring the pole width of $X(3872)$ and the characteristics of the higher resonance in fully resolving the puzzle of $X(3872)$. By matching the predicted resonance to the newly observed $\chi_{c1}(4010)$, we conclusively identify the $D\bar{D}^*$ pole as the origin of $X(3872)$ with overwhelming confidence.

Note added. About one month after this work was posted on arXiv, we notice that the LHCb Collaboration released the amplitude analysis results of $B^+ \to D^{*\pm}D^{\mp}K^+$ and observed a new charmoniumlike state $\chi_{c1}(4010)$ with quantum number $J^{PC} = 1^{++}$ decaying into $D^{*\pm}D^{\mp}$, whose mass and width are fitted to be $4012.5^{+3.6+4.1}_{-2.9-3.7}$ and $62.7^{+7.0+6.4}_{-6.4-6.6}$ MeV [63], respectively. The newly observed $\chi_{c1}(4010)$ surprisingly coincides with our predicted higher resonance around 4.0 GeV, which strongly supports the key role of the coupled channel dynamics in the formation of $X(3872)$.

Acknowledgments. This work is supported by the National Science Foundation of China under Grants No. 11975033, No. 12070131001, No. 12147168, No. 12475137, and No. 12405088. This project was also funded by the Deutsche Forschungsgemeinschaft (DFG, German Research Foundation, Project ID 196253076-TRR 110). J.-Z. W. is also supported by the National Postdoctoral Program for Innovative Talent. The computational resources were supported by High-performance Computing Platform of Peking University.

[1] H.-X. Chen, W. Chen, X. Liu, and S.-L. Zhu, Phys. Rep. **639**, 1 (2016).
[2] Y.-R. Liu, H.-X. Chen, W. Chen, X. Liu, and S.-L. Zhu, Prog. Part. Nucl. Phys. **107**, 237 (2019).
[3] F.-K. Guo, C. Hanhart, U.-G. Meißner, Q. Wang, Q. Zhao, and B.-S. Zou, Rev. Mod. Phys. **90**, 015004 (2018); **94**, 029901(E) (2022).
[4] N. Brambilla, S. Eidelman, C. Hanhart, A. Nefediev, C.-P. Shen, C. E. Thomas, A. Vairo, and C.-Z. Yuan, Phys. Rep. **873**, 1 (2020).
[5] S. L. Olsen, T. Skwarnicki, and D. Zieminska, Rev. Mod. Phys. **90**, 015003 (2018).
[6] L. Meng, B. Wang, G.-J. Wang, and S.-L. Zhu, Phys. Rep. **1019**, 1 (2023).
[7] S. K. Choi *et al.* (Belle Collaboration), Phys. Rev. Lett. **91**, 262001 (2003).
[8] G. Gokhroo *et al.* (Belle Collaboration), Phys. Rev. Lett. **97**, 162002 (2006).
[9] M. B. Voloshin, Phys. Lett. B **579**, 316 (2004).
[10] E. Braaten and M. Kusunoki, Phys. Rev. D **69**, 074005 (2004).
[11] E. S. Swanson, Phys. Lett. B **588**, 189 (2004).
[12] N. A. Tornqvist, Phys. Lett. B **590**, 209 (2004).
[13] S. Fleming, M. Kusunoki, T. Mehen, and U. van Kolck, Phys. Rev. D **76**, 034006 (2007).
[14] Y.-R. Liu, X. Liu, W.-Z. Deng, and S.-L. Zhu, Eur. Phys. J. C **56**, 63 (2008).
[15] R. Aaij *et al.* (LHCb Collaboration), Nat. Phys. **18**, 751 (2022).
[16] R. Aaij *et al.* (LHCb Collaboration), Nat. Commun. **13**, 3351 (2022).
[17] A. V. Manohar and M. B. Wise, Nucl. Phys. **B399**, 17 (1993).
[18] D. Janc and M. Rosina, Few Body Syst. **35**, 175 (2004).
[19] S. Ohkoda, Y. Yamaguchi, S. Yasui, K. Sudoh, and A. Hosaka, Phys. Rev. D **86**, 034019 (2012).
[20] N. Li, Z.-F. Sun, X. Liu, and S.-L. Zhu, Phys. Rev. D **88**, 114008 (2013).
[21] K. Chen, R. Chen, L. Meng, B. Wang, and S.-L. Zhu, Eur. Phys. J. C **82**, 581 (2022).
[22] X.-K. Dong, F.-K. Guo, and B.-S. Zou, Commun. Theor. Phys. **73**, 125201 (2021).
[23] A. Feijoo, W. H. Liang, and E. Oset, Phys. Rev. D **104**, 114015 (2021).
[24] M. Albaladejo, Phys. Lett. B **829**, 137052 (2022).
[25] S. Fleming, R. Hodges, and T. Mehen, Phys. Rev. D **104**, 116010 (2021).
[26] L. Meng, G.-J. Wang, B. Wang, and S.-L. Zhu, Phys. Rev. D **104**, 051502 (2021).
[27] M.-L. Du, V. Baru, X.-K. Dong, A. Filin, F.-K. Guo, C. Hanhart, A. Nefediev, J. Nieves, and Q. Wang, Phys. Rev. D **105**, 014024 (2022).
[28] Z.-Y. Lin, J.-B. Cheng, and S.-L. Zhu, Phys. Rev. D **110**, 054008 (2024).
[29] J.-B. Cheng, Z.-Y. Lin, and S.-L. Zhu, Phys. Rev. D **106**, 016012 (2022).
[30] H.-W. Ke, X.-H. Liu, and X.-Q. Li, Eur. Phys. J. C **82**, 144 (2022).
[31] X.-Z. Ling, M.-Z. Liu, L.-S. Geng, E. Wang, and J.-J. Xie, Phys. Lett. B **826**, 136897 (2022).
[32] Y. Liu, M. A. Nowak, and I. Zahed, Phys. Rev. D **105**, 054021 (2022).
[33] M.-J. Yan and M. P. Valderrama, Phys. Rev. D **105**, 014007 (2022).
[34] Y. Jin, S.-Y. Li, Y.-R. Liu, Q. Qin, Z.-G. Si, and F.-S. Yu, Phys. Rev. D **104**, 114009 (2021).
[35] Q. Xin and Z.-G. Wang, Eur. Phys. J. A **58**, 110 (2022).
[36] J. Shi, E. Wang, and Q. Wang, Phys. Rev. D **106**, 096012 (2022).
[37] P. G. Ortega, J. Segovia, D. R. Entem, and F. Fernandez, Phys. Lett. B **841**, 137918 (2023); **847**, 138308(E) (2023).
[38] M.-L. Du, A. Filin, V. Baru, X.-K. Dong, E. Epelbaum, F.-K. Guo, C. Hanhart, A. Nefediev, J. Nieves, and Q. Wang, Phys. Rev. Lett. **131**, 131903 (2023).
[39] J.-Z. Wang, Z.-Y. Lin, and S.-L. Zhu, Phys. Rev. D **109**, L071505 (2024).
[40] B. Wang and L. Meng, Phys. Rev. D **107**, 094002 (2023).
[41] C. Chen, C. Meng, Z. Xiao, and H.-Q. Zheng, Chin. Phys. C **48**, 043102 (2024).
[42] R. Chen, Q. Huang, X. Liu, and S.-L. Zhu, Phys. Rev. D **104**, 114042 (2021).
[43] R. Aaij *et al.* (LHCb Collaboration), Phys. Rev. Lett. **110**, 222001 (2013).
[44] R. Aaij *et al.* (LHCb Collaboration), Phys. Rev. D **92**, 011102 (2015).
[45] V. Baru, C. Hanhart, Y. S. Kalashnikova, A. E. Kudryavtsev, and A. V. Nefediev, Eur. Phys. J. A **44**, 93 (2010).
[46] C. Hanhart, Y. S. Kalashnikova, and A. V. Nefediev, Eur. Phys. J. A **47**, 101 (2011).
[47] I. K. Hammer, C. Hanhart, and A. V. Nefediev, Eur. Phys. J. A **52**, 330 (2016).
[48] C. Hanhart and A. Nefediev, Phys. Rev. D **106**, 114003 (2022).
[49] M. R. Pennington and D. J. Wilson, Phys. Rev. D **76**, 077502 (2007).
[50] S. Ono and N. A. Tornqvist, Z. Phys. C **23**, 59 (1984).
[51] B.-Q. Li, C. Meng, and K.-T. Chao, Phys. Rev. D **80**, 014012 (2009).
[52] Z.-Y. Zhou and Z. Xiao, Eur. Phys. J. A **50**, 165 (2014).
[53] M.-X. Duan, S.-Q. Luo, X. Liu, and T. Matsuki, Phys. Rev. D **101**, 054029 (2020).
[54] Q. Deng, R.-H. Ni, Q. Li, and X.-H. Zhong, Phys. Rev. D **110**, 056034 (2024).
[55] Z.-L. Man, C.-R. Shu, Y.-R. Liu, and H. Chen, Eur. Phys. J. C **84**, 810 (2024).
[56] J. A. Oller, E. Oset, and J. R. Pelaez, Phys. Rev. D **59**, 074001 (1999); **60**, 099906(E) (1999); **75**, 099903(E) (2007).
[57] S. Godfrey and N. Isgur, Phys. Rev. D **32**, 189 (1985).
[58] T. Barnes, S. Godfrey, and E. S. Swanson, Phys. Rev. D **72**, 054026 (2005).
[59] See Supplemental Material at http://link.aps.org/supplemental/10.1103/929g-cv15 for additional details on the pole trajectories of the $D\bar{D}^*$ scattering including the intrinsic $D\bar{D}^*$ dynamics, the experimental constraints on the pole positions of $X(3872)$ and the predicted new resonance, the uniformization in the two-channel problem, the nonopen charm and open charm decay behaviors of χ_{c1}', the three-body threshold dynamics and the self-energy effect of $\bar{D}^*$ in the $D\bar{D}^*$ scattering, and the pole behaviors of the full $D\bar{D}^*$

scattering dynamics by considering the isospin violation of the contact potential, which include Refs. [27,28,39,60–73].
[60] R. L. Workman *et al.* (Particle Data Group), Prog. Theor. Exp. Phys. **2022**, 083C01 (2022).
[61] R. Aaij *et al.* (LHCb Collaboration), Phys. Rev. D **102**, 092005 (2020).
[62] M. Ablikim *et al.* (BESIII Collaboration), Phys. Rev. Lett. **132**, 151903 (2024).
[63] R. Aaij *et al.* (LHCb Collaboration), Phys. Rev. Lett. **133**, 131902 (2024).
[64] F. E. Close and E. S. Swanson, Phys. Rev. D **72**, 094004 (2005).
[65] D. Guo, J.-Z. Wang, D.-Y. Chen, and X. Liu, Phys. Rev. D **106**, 094037 (2022).
[66] W. Kwong, P. B. Mackenzie, R. Rosenfeld, and J. L. Rosner, Phys. Rev. D **37**, 3210 (1988).
[67] W. Kwong and J. L. Rosner, Phys. Rev. D **38**, 279 (1988).
[68] V. A. Novikov, L. B. Okun, M. A. Shifman, A. I. Vainshtein, M. B. Voloshin, and V. I. Zakharov, Phys. Rep. **41**, 1 (1978).
[69] L. Micu, Nucl. Phys. **B10**, 521 (1969).
[70] A. Le Yaouanc, L. Oliver, O. Pene, and J. C. Raynal, Phys. Rev. D **8**, 2223 (1973).
[71] V. Bhardwaj *et al.* (Belle Collaboration), Phys. Rev. Lett. **107**, 091803 (2011).
[72] R. Aaij *et al.* (LHCb Collaboration), Nucl. Phys. **B886**, 665 (2014).
[73] M. Mai, B. Hu, M. Doring, A. Pilloni, and A. Szczepaniak, Eur. Phys. J. A **53**, 177 (2017).
[74] W. Yamada and O. Morimatsu, Phys. Rev. C **102**, 055201 (2020).
[75] W. A. Yamada, O. Morimatsu, T. Sato, and K. Yazaki, Phys. Rev. D **105**, 014034 (2022).
[76] L. Meng, B. Wang, and S.-L. Zhu, Phys. Rev. D **107**, 014005 (2023).
[77] D. Morel and S. Capstick, arXiv:nucl-th/0204014.
[78] P. G. Ortega, J. Segovia, D. R. Entem, and F. Fernandez, Phys. Rev. D **94**, 074037 (2016).
[79] Z. Yang, G.-J. Wang, J.-J. Wu, M. Oka, and S.-L. Zhu, Phys. Rev. Lett. **128**, 112001 (2022).
[80] J. Aguilar and J. M. Combes, Commun. Math. Phys. **22**, 269 (1971).
[81] E. Balslev and J. M. Combes, Commun. Math. Phys. **22**, 280 (1971).
[82] T. Myo, Y. Kikuchi, H. Masui, and K. Katō, Prog. Part. Nucl. Phys. **79**, 1 (2014).
[83] W. J. Romo, Nucl. Phys. **A116**, 617 (1968).
[84] Z.-Y. Lin, J.-B. Cheng, B.-L. Huang, and S.-L. Zhu, Phys. Rev. D **108**, 114014 (2023).
[85] Y. S. Kalashnikova, Phys. Rev. D **72**, 034010 (2005).
[86] S. Coito, G. Rupp, and E. van Beveren, Eur. Phys. J. C **73**, 2351 (2013).
[87] E. Cincioglu, J. Nieves, A. Ozpineci, and A. U. Yilmazer, Eur. Phys. J. C **76**, 576 (2016).
[88] Z.-Y. Zhou and Z. Xiao, Phys. Rev. D **96**, 054031 (2017); **96**, 099905(E) (2017).
[89] F. Giacosa, M. Piotrowska, and S. Coito, Int. J. Mod. Phys. A **34**, 1950173 (2019).
[90] G.-J. Wang, Z. Yang, J.-J. Wu, M. Oka, and S.-L. Zhu, Sci. Bull. **69**, 3036 (2024).
[91] H. Li, C. Shi, Y. Chen, M. Gong, J. Liang, Z. Liu, and W. Sun, arXiv:2402.14541.